The confinement analysis in ST40 spherical tokamak

A. Dnestrovskii, A. Sladkomedova, J. Varje, M. Sertoli, H. Lowe, M. Gemmell, M. Iliasova, X.Zhang and the ST40 Team

Tokamak Energy Ltd, Oxfordshire OX14 4SD, UK

The dependence of plasma energy confinement time on the magnetic field was demonstrated to be much stronger in spherical tokamaks (STs), such as MAST, NSTX and GLOBUS-M2, than in conventional tokamaks with high aspect ratio A>2.5 [1]. The maximum toroidal field achieved in those STs was 0.9 T [2] and, therefore, to be applicable for future ST-based fusion devices with a foreseen toroidal field of 4-5 T, extrapolation of the ST confinement scaling law is required.

Experiments on the high-field spherical tokamak ST40 [3,4] with NBI heated plasmas of 1 MW/55 keV of power/energy were carried out, with a toroidal magnetic field at the geometric axis varying between 0.6 T and 1.7 T, in L- and ELM-free H- modes plasmas with two values of plasma current 390kA and 500kA. All plasmas were diverted, sawteeth oscillated and reached its steady state of longer than estimated confinement time duration where time of interest was chosen. Specific features of scenario are different in L- and H- models. In L-mode the electron density measured by both Thomson Scattering (TS) and interferometer does not change much in a time. After the L-H transition electron density starts to increase in time without saturating. The density behaviour is rather similar between shots reaching roughly $8\cdot10^{19}m^{-3}$ with 20% scattering during the time of interest between 0.1s and 0.13s. The Argon puffing was used as a tool to avoid L-H transition, so that H-mode regularly reached in shots without Argon puffing. The electron temperature increased with the rise of the toroidal magnetic field. Electron density profiles measured by TS in L-mode are regularly more peaked than in H-mode where the pedestal values around $4\text{-}6\cdot10^{19}m^{-3}$ are clearly seen. Electron temperature profile is flat in the central plasma revealing the impact of sawteeth, and without clearly seen pedestals in the H-mode. The ion temperature measured by chord emission of X-ray Ar line (XRCS) shows the less expressed rise with the field than Te. The lower Argon emission in H-mode series results in higher error bars of Ti measurements than in L-mode.

The stored energy measured by the diamagnetic signal is obtained to increase with the field in both L and H mode series as shown in figure 1. The similar behaviour is seen in figure 2 for a neutron flux measured by a diamond detector but only for L-mode series. For H-mode plasmas neutron flux is lower and regular data were not obtained. The NPA data show a strong correlation with SXR sawteeth oscillations in figure 3 revealing the fast particle losses during the sawtooth crash.

Model for the interpretative analysis

In our analysis we use the ASTRA transport code [5] together with the NUBEAM code [6] for calculation of the NBI heating power and fast particle fraction. Plasma boundary is reconstructed from magnetic data using EFIT code and is used in SPIDER [7] code for a fixed boundary equilibrium calculation. Interpretation analysis uses TS measured electron density and temperature profiles. The energy confinement time is calculated with the formula

$$\tau_E = \frac{W_{th}}{P_{Ohm} + P_{abs}^{NBI} - \frac{dW_{th}}{dt}}$$

where W_{th} is the thermal energy and P_{Ohm} and $P_{abs}{}^{NBI}$ are the Ohmic and NBI absorbed power. Z_{eff} =2.5 is taken to be uniform over the radius with the equal contribution from Ar and C, no radiation is included to the model and steady state time of interest is taken.

Main uncertainties of the model are going from defining neutral density, Ti profile and fast particle losses. Deuterium neutral density uncertainty is introduced in the model by estimating the neutral density at the plasma boundary between 10^{16} and 10^{17} m^{-3} from D_α line emission. Ti profile is calculated using the heat conductivity coefficient containing ion neoclassical term and anomalous term:

$$\chi_{ion} = \chi_{ion,neocl} + C_1 \cdot (1 + C_2 \rho^5)$$

where C_1 is a numerical coefficient used to fit the experimental XRCS signal and C_2 is used to introduce T_i profile uncertainty to the result. With the experimental constraint Ti profiles with lower central temperature gives higher value of ion thermal energy and higher value of the energy confinement time. Figure 4 shows two limiting Ti profiles corresponding to C_2=0 and 20. It is obtained that any other variation of ion heat conductivity with the condition to be above the ion neoclassical conductivity does not produce much larger uncertainty in the answer.

Introducing anomalous losses of fast particles strongly affects the result. We consider anomalous losses are caused by sawteeth mixing inside q=1 surface pushing fast particles to a periphery plasma where the charge-exchange and bad-orbit losses are taken place. In the model the anomalous diffusion coefficient for fast particles is set D_{FP}=1 m^2/s. Figure 5 shows that the effect of these losses on a total absorbed power is more pronounced in lower field shots which is the result of increasing radius of q=1 surface toward this direction. As it is said above NPA data give strong evidence of fast particle losses during the sawtooth crash. Neutron flux data shown in figure 2 give also some evidence of introduction the fast particle losses: calculations with fast particle losses show that the slope over the magnetic field is closer to the slope of the measured data. The same argument can be implemented when comparing the total stored energy with the diamagnetic data.

The effect of uncertainties is demonstrated in comparison to a *reference* case with $10^{16}m^{-3}$ for the edge neutral density, C_2=0 and D_{FP}=0.

Table 1 Results of confinement time fitting

	H-mode	L-mode
Existing scaling	$\tau_E^{IPB(y,2)} \sim B_t^{0.15} n_e^{0.4}$ [8] $\tau_E^{Globus\text{-}M2} \sim B_t^{1.05} n_e^{0.65}$ [1]	$\tau_E^{IPB(L\text{-}mode)} \sim B_t^{0.03} n_e^{0.4}$ [8]
τ_E^{ST40}	$B_t^{0.76} n^{0.5}$ for B_t<1.1T $I_p^{0.9} n^{0.5}$ for B_t>1.1T	$B_t^{0.32} n^{0.4}$

Main results

Calculated energy confinement time for three series and exponential fittings are shown in figure 6. Error bars include measured Ti errors from XRCS Argon line and modelling uncertainties mentioned above: neutral density, Ti-profile and fast particle losses. For L-mode error bars decrease with the rise of magnetic field because of the fast particle loss uncertainty has less impact on the result. Higher error bars in high current H-mode case reflect the contribution of measured errors.

For H-mode lower current case the increase of the confinement time is clearly at the low field seen to saturate B_t ~1.1T. For B_t > 1.1T the increase of confinement time is not seen. We can also see the increase of confinement time with the plasma current between two H-mode series with different plasma current. For L-mode series the increase of the confinement time is seen over all range of the field without saturation.

Without density control the same scenario of gas puffing results in the density values correlating with the particle confinement time. Figure 7 shows the dependence of electron density on the magnetic field similar to the confinement time dependence meaning the particle and thermal confinement times are correlated. To determine the energy confinement time dependence on separately on the magnetic field and on the density the additional density scan with a different particle source is needed for the same other conditions. Here we can use a benefit of density exponents in different existing confinement time scalings. Table 1 shows the results of ST40 confinement time fittings with prescribed density dependence exponent 0.5 in H-mode and 0.4 in L-mode.

Saturation of the energy confinement time rise for B_t > 1.1T in H-mode shots can be caused by the increase of magnetic perturbations activity in the frequency range 50-100kHz shown in figure 8. The identification of this microturbulence modes is the subject of gyro-kinetic analysis that is outside of the paper. L-mode branch is different: no increase in magnetic perturbations and no confinement saturation are seen

Conclusions

- In H-mode 390kA series it is clearly seen that confinement increase saturates when B_t >1.1T
- Saturation of confinement rise with B_t in H-mode shots can be caused by the increase of magnetic perturbations activity in the frequency range 50-100kHz.
- In H-mode 500kA series it is unclear if confinement saturates because of missing discharges at low field
- H-mode plasma with I_p 390kA and 500kA series is close to IPB(y,2) scaling when B_t >1.1T
- Confinement time is obtained to be below the Globus-M2 scaling for STs but for lower field region shows similar dependence on the magnetic field. Note that no radiation is included to calculations.
- The increase of confinement with the plasma current is clearly seen
- In L-mode the stronger field dependence TauE ~ $B_t^{0.32}n^{0.4}$ than in IPB scaling $TauE^{IPB(L\text{-}mode)}$ ~ $B_t^{0.03}n^{0.4}$ and no saturation of confinement is obtained.

References

1. G.S. Kurskiev *et al* 2022 *Nucl. Fusion* **62** 016011
2. G. S. Kurskiev, *et al* 2024 Phys. Plasmas 31, 062511
3. S. McNamara et al., 2023 Nuclear Fusion 63 054002
4. O. Asunta et al 2026 Nucl. Fusion 66 116004
5. G.V. Pereverzev and P.N. Yushmanov, 2002 IPP Report 5/98
6. A. Pankin et al., 2004 Comput. Phys. Commun. 159 157–84
7. A.A. Ivanov et al 2005 32nd EPS Conf. on Plasma Physics vol 29C (ECA) P-5.063
8. ITER Physics Expert Group on Confinement and Transport, 1999 Chapter 2: plasma confinement and transport Nucl. Fusion 39 2175

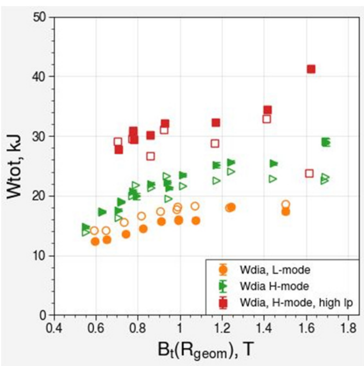

Figure 1 Stored energy for L-mode series (orange circles) H-mode (green triangles) and H-mode higher current (red squares) measured by diamagnetic signal (filled symbols) and obtained in a reference case but including fast particle losses: D_{FP}=1 m^2/s (open symbols)

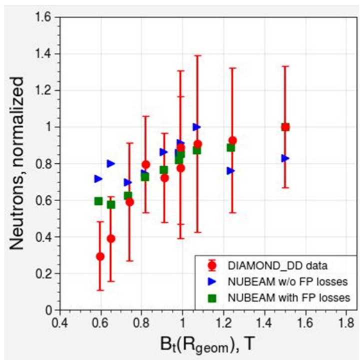

Figure 2 Normalized neutron flux measured by diamond detector (red circles) and obtained in calculations for reference case (blue triangles) and with fast particle losses (green squares)

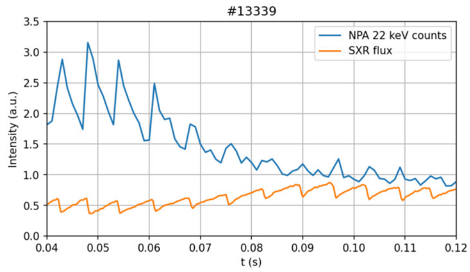

Figure 3 Time evolution of NPA signal for one of the L-mode shots and SXR data. Sawtooth crash correlates with the jump of NPA showing the increase of fast particle losses.

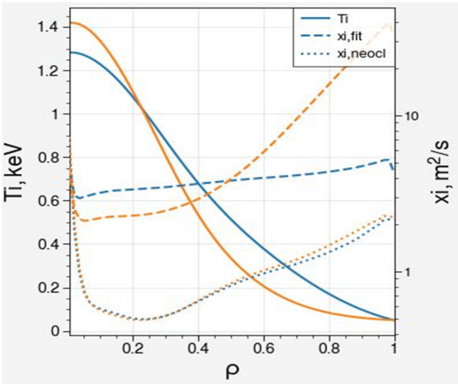

Figure 4 Ion temperature profiles, heat ion conductivity (dashed line) and ion neoclassical heat conductivity (dotted line) in a reference run (blue) and peaked Ti run (orange) calculated for shot #13669.

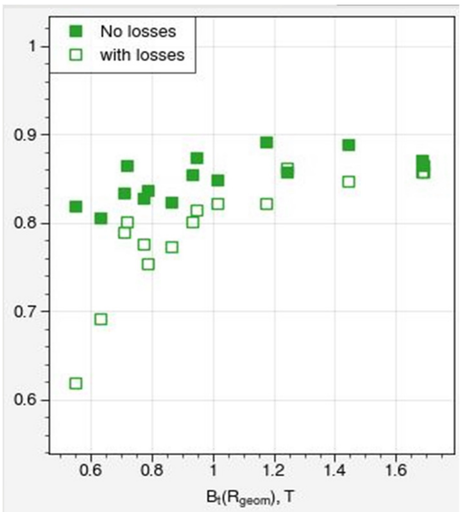

Figure 5 Absorbed NBI power calculated with NUBEAM code for the reference case (filled squares) and for the case with increased fast particle losses (open squares) for the L-mode series.

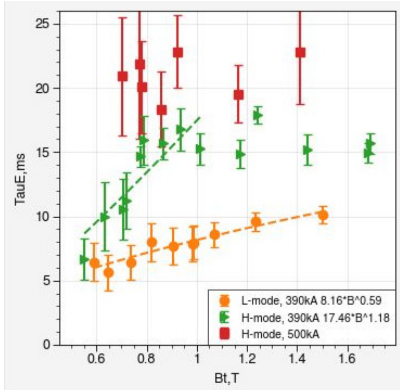

Figure 6 Calculated energy confinement time for L-mode series (orange) H-mode (green) and H-mode higher current (red) and exponential fittings

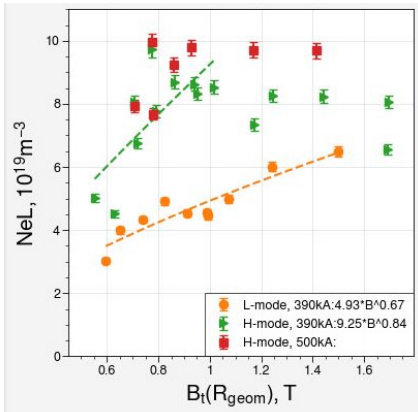

Figure 7 Line averaged electron density for L-mode series (orange) H-mode (green) and H-mode higher current (red) measured by interferometer (filled symbols) and exponential fittings

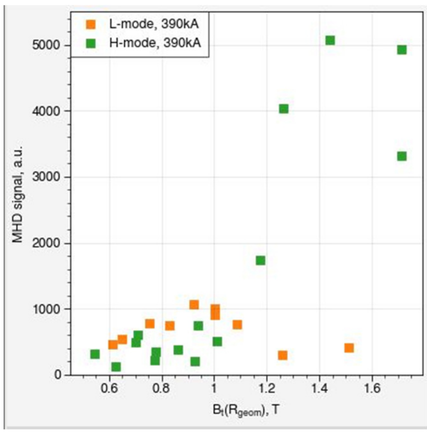

Figure 8 Energy of magnetic perturbations taken from Mirnov probe at the outboard midplane averaged over a frequency range 50-100kHz for L-mode series (orange) and H-mode series (green)